Properties of a Glass-Forming System as Derived from Its Potential Energy Landscape

Andreas Heuer
Max-Planck-Institut für Polymerforschung, Ackermannweg 10, D-55128 Mainz, Germany
(Received 23 December 1996)

Many properties of glass-forming systems can be explained in terms of their multidimensional potential energy landscape. Here the total potential energy landscape of a small glass-forming system with periodic boundary conditions is determined numerically. An appropriate one-dimensional projection is introduced. It allows one to visualize how crystalline and amorphous regions are separated from each other and to find a direct explanation of prominent dynamic features observed in molecular dynamics simulations. The energy landscape and the occurrence of tunneling systems is elucidated for different densities. [S0031-9007(97)03185-2]

PACS numbers: 61.43.Fs, 64.70.Pf, 82.20.Wt

The properties of glasses at very low temperatures (Kelvin regime) are typically described by postulating the existence of tunneling systems [1,2]. They can be envisaged as localized groups of atoms or molecules cooperatively moving between two configurations with comparable energy [3,4]. Also the dynamics around the glass transition temperature T_g is often related to cooperative jump processes [5,6]. For rationalizing the properties of glass-forming systems close to T_g and below, many authors have used the concept of the multidimensional potential energy landscape in configuration space [5,7–17]. The dynamical processes can be interpreted as transitions between adjacent local minima. Also for the analysis of proteins the concept of an energy landscape has become an important tool [18]. In contrast, the mode-coupling theory describes the onset of freezing from the liquid state [19].

Qualitatively, the energy landscape of glass-forming systems is usually sketched as a 1D potential containing a large number of hills and valleys [20]; see Fig. 1(a). The crystalline state corresponds to the lowest energy minimum, here minimum A. In order to obtain a *quantitative* version of Fig. 1(a), two steps are involved. First, one has to fully characterize the high-dimensional energy landscape; second, one has to find an appropriate projection scheme on a 1D potential. Since to the best of our knowledge no general projection scheme exists, presentation of 1D potentials is mainly of qualitative value.

Analysis of the total energy landscape requires numerical simulations. For small spin glass clusters the energy landscape has been calculated already many years ago [21]. In recent years, progress has been achieved in determining the *total* energy landscape of small noble gas clusters with at most 13 atoms [22,23]. Since the number of minima exponentially grows with the number of particles, extension to larger clusters is not possible in a complete way [17,24,25]. Obviously, the physical properties of small clusters are largely dominated by surface effects. If one is interested in the simulation of bulklike properties or pressure effects for small systems it is essential to use periodic boundary conditions.

For the first time we determine the total energy landscape of a glass-forming system with periodic boundary conditions and introduce a projection scheme on a 1D potential which keeps relevant features (to be specified below) of the high-dimensional potential. From the 1D potential, information is accessible which allows direct interpretation of features seen in MD simulations in the supercooled regime [7]. Furthermore, direct connection of the energy landscape to the low-temperature anomalies is possible.

The whole procedure is exemplified for a Lennard-Jones– (LJ-) type model system taken from the work of Stillinger and Weber [7], containing 32 particles. The simulated densities are $\rho = 1$ and $\rho = 1.075$ in units of the nearest-neighbor distance a and unit mass. For a polymer glass the density difference corresponds to an applied pressure of approximately 4 kbar [26]. The energy of the fcc crystal $E_{\text{cryst}}(\rho)$ has its minimum for $\rho = 1$ [$E_{\text{cryst}} \equiv E_{\text{cryst}}(\rho = 1) = -192$ in LJ units [7]]. The analysis of different densities is motivated by the experimental observation that the density of tunneling systems in a glassy polymer significantly decreases upon application of pressure [26].

In a first step, about 10^5 conjugate gradient minimization procedures, starting from arbitrarily chosen initial configurations, were performed in order to get a (hopefully) complete list of energy minima $E(k)$. We found 367 minima with different energy for $\rho = 1$ and 75 for

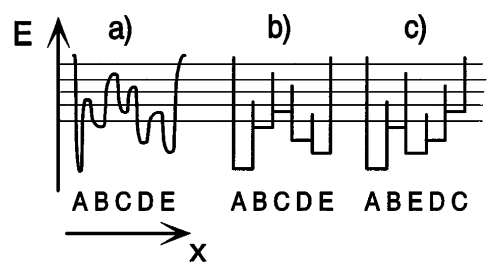

FIG. 1. (a) A simple 1D energy landscape, (b) a schematic representation of (a), (c) the potential minima are rearranged. In all cases the transfer matrix $\tilde{V}(k_1, k_2)$ is identical. The horizontal lines are discussed in the text.

$\rho = 1.075$. Their distribution is plotted in Fig. 2. The number for $\rho = 1$ is approximately twice as large as previously reported for the identical model [7], showing that high-energy minima are rather difficult to detect. Whereas the crystalline minimum turns out to be stable upon increasing density, this does not hold for most amorphous minima. This is already reflected by the observation that the absolute number of minima decreases by more than a factor of 4 when going from $\rho = 1$ to $\rho = 1.075$ (see Ref. [27] for a similar result). Performing the minimization with *variable* density we observed that the number of different minima dramatically increases so that a systematic search is no longer possible. This partly explains the observation of why the number of energy minima of 13 particles in a cluster with no constraints on density is of the same order as that of 32 particles in a fixed volume.

In a second step, we determined the distances of all pairs (k_1, k_2) of minima in configuration space. If the positions of the N particles are given by $\{\vec{r}_{i_1,k_1}\}$ and $\{\vec{r}_{i_2,k_2}\}$, one can define the Euclidean distance by

$$[d(k_1, k_2)]^2 = \sum_{i_1=1}^{N} [\vec{r}_{i_1,k_1} - \vec{r}_{i_2(i_1),k_2}]^2. \tag{1}$$

The notation $i2(i1)$ indicates that *a priori* it is not evident which particle of configuration k_2 corresponds to which particle of k_1, so that several mappings have to be checked. For application of Eq. (1), two further aspects have to be considered. First, due to the periodic boundary conditions the configuration $\{\vec{r}_{i,k_j}\} + \vec{a}_j$ with arbitrary vector $\vec{a}_j$ also belongs to energy minimum k_j. Hence for an appropriate definition of $d(k_1, k_2)$ one additionally has to determine the value of $\vec{a}_1 - \vec{a}_2$ which minimizes $d(k_1, k_2)$. Second, for a 3D cube, one minimum corresponds to 48 different configurations which are related by symmetry operations like 90° rotations. This number results from 3! permutations of axes and 2^3 reflections. Hence a comparison of two energy minima in reality corresponds to a comparison of one configuration belonging to k_1 with 48 symmetry related configurations belonging to k_2. For the determination of $d(k_1, k_2)$, we calculated the distance for all symmetry related configurations and chose the minimum value. Since the MD simulations in [7] revealed that for ambient temperatures only configurations with $E(k) < (5/6)E_{\text{cryst}}$ are relevant, we restricted our analysis to these 223 minima. For $\rho = 1.075$ we analyzed all minima. Preliminary MD studies show that adjacent amorphous minima in configuration space tend to have a distance of $d \leq 2$ (in LJ units) [28].

For a given configuration k_1, we define $d_{\min}(k_1) = \min_{k2} d(k_1, k_2)$. This value is a measure of how close the relevant configurations are in the high-dimensional configuration space. In Fig. 3 the distribution of $d_{\min}^2$ is plotted for both densities. In agreement with intuition in both cases the configuration with the largest value of $d_{\min}$ corresponds to the crystalline structure. Interestingly, for $\rho = 1.075$ the whole $d_{\min}$ distribution is shifted to larger values, yielding a gap for $d_{\min} < 0.6$. Hence for denser systems the different configurations are farther away from each other in configuration space. As shown in previous work, the tunneling systems which dominate the low temperature properties correspond to pairs of minima with an average value of $d \approx 0.35$ [29]. Hence the present calculations, at least qualitatively, predict a significant decrease of the tunneling systems with increasing pressure in agreement with experiment [26].

The energies $V(k_1, k_2)$ at the saddles were estimated as follows. In the soft potential model the reaction path between adjacent energy minima is parametrized by quartic polynomials of the type $w_2(x/a)^2 - w_3(x/a)^3 + w_4^0(x/a)^4$ with constant w_4^0 and independently distributed w_2 and w_3 (x: Euclidean distance along the reaction path, a equilibrium nearest-neighbor distance) [30]. Recent simulations have shown $w_4^0 \approx 10$ (in LJ units) [31]. Postulating that w_4^0 describes the quartic term of the transition between all pairs of adjacent minima, the values of w_2 and w_3 and thus of $V(k_1, k_2)$ can be directly estimated from knowledge of $d(k_1, k_2)$ and the energies $E(k_1), E(k_2)$. For pairs of minima with $d(k_1, k_2) > 2$ we formally set $V(k_1, k_2) = \infty$. The subsequent results are insensitive to the precise value of w_4^0 and to the definition of adjacent minima ($d \leq 2$).

The information about the energy landscape is expressed by the energies $E(k)$, the distance $d(k_1, k_2)$, and the saddle point energies $V(k_1, k_2)$. In the spirit of the work of Stillinger [11], we also define the *transfer matrix* $\tilde{V}(k_1, k_2)$

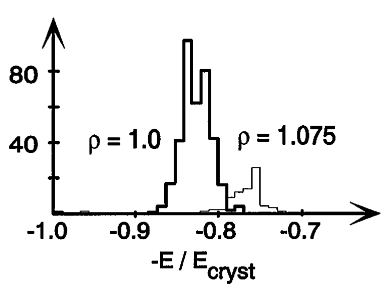

FIG. 2. The energy distribution of minima for $\rho = 1$ (thick line) and $\rho = 1.075$ (thin line).

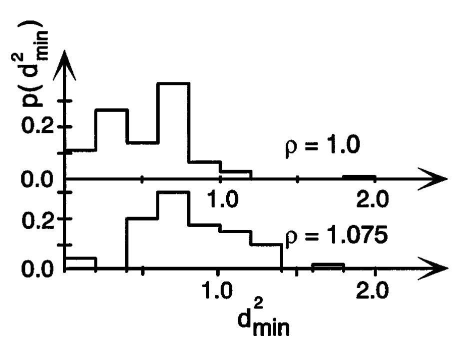

FIG. 3. The distribution of the value $d_{\min}^2$ for $\rho = 1$ (upper curve) and $\rho = 1.075$ (lower curve). Note the depopulation of small values of $d_{\min}^2$ for $\rho = 1.075$.

which contains the minimum saddle point energy for all (indirect and direct) paths from minimum k_1 to minimum k_2. This matrix expresses the connectivity among all minima. As discussed in [11], $\tilde{V}(k_1, k_2)$ contains important information about the dynamics in glass-forming systems and is the basis for the definition of metabasins. For a 1D potential, the $\tilde{V}(k_1, k_2)$ are easily determined because minima k_1 and k_2 are connected by only a single path. Now we show that for arbitrary multidimensional potentials it is possible to construct a 1D potential with an *identical* transfer matrix. This enables visualization of important information in 1D and, furthermore, gives a strict recipe of how 1D representations of multidimensional potentials may be interpreted.

The algorithm can be outlined as follows. For given energy E_0 we form groups of minima. A group is defined such that $\tilde{V}(k_1, k_2) \leq E_0$ for all members of one group and $\tilde{V}(k_1, k_2) > E_0$ otherwise ($k_1 \neq k_2$). For $E_0 \rightarrow \infty$ one has a single group which, during a decrease of E_0, continuously splits into smaller groups. For $E_0 \rightarrow -\infty$ no group is left. From checking all different E_0, indicated in Fig. 1 as horizontal lines, the different groups for the potential in Fig. 1(a) read (A,B,C,D,E), (A,B), (C,D,E), (D,E). One can easily convince oneself that it is possible for arbitrary multidimensional potentials to sort all minima $k_1, \ldots, k_N$ such that all the members of any group are contiguous. For the potential of Fig. 1 this is fulfilled for, e.g., ABCDE and ABEDC but not for, e.g., ABECD, since here the members of the group (D,E) are not contiguous. Based on this sorting the schematic potentials, shown in Figs. 1(b) and 1(c), can be constructed with identical $\tilde{V}(k_1, k_2)$ as the original (possibly multidimensional) potential. In order to have a unique representation, we further require that, starting from the left, the sequence of energy minima increases as monotonically as possible; see Fig. 1(c). Note that bins which are adjacent in the 1D projection may have a large distance in the real potential landscape like minima B and E in Fig. 1(c).

In Fig. 4 this schematic potential is shown for the energy landscape of the LJ glass with $\rho = 1$. First, one can see the isolated crystalline minimum on the left side. A very high energy has to be reached before the crystal can "melt." A precise description of melting, however, is beyond the scope of this Letter. For the noncrystalline minima, basically two regions I and II can be distinguished, region I containing minima 3–6 (only minimum 3, having an energy of $E(3)/E_{\text{cryst}} \approx 0.895$, is relevant), region II the other relevant amorphous minima. From knowledge of the energy landscape one may predict that the longest time scale of relaxation at low temperatures is related to the transition between both noncrystalline regions I and II and that the time to leave minimum 3 is longer than for other minima. This nontrivial prediction is in agreement with the MD simulations of Stillinger and Weber (see Fig. 5 of [7]) and confirmed by MD simulations in our group [28]. It has been even shown that the value of the low-temperature activation energy of the density-density correlation function roughly agrees with the barrier height between regions I and II ($\approx$6 in LJ units). Closer inspection shows that minimum 3 has some intrinsic symmetries indicating that this minimum is not purely amorphous.

In the remaining part, we extract the information content of the energy landscape about the low-temperature anomalies. We start by identifying double well potentials (DWPs). We define a DWP as adjacent pairs of minima k_1 and k_2 such that the energy at its saddle is smaller than the energy of all other saddles which can be reached

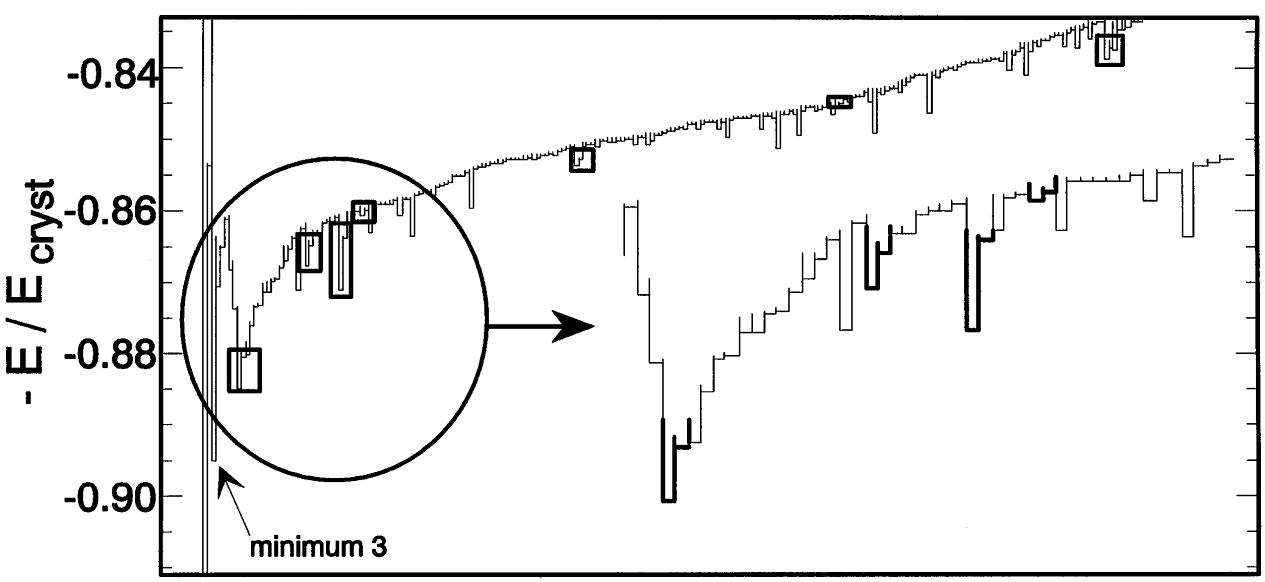

FIG. 4. The energy landscape for $\rho = 1$. The double well potentials and minimum 3 are highlighted. All minima with energy $E < (5/6)E_{\text{cryst}}$ are included.

either from minimum k_1 or k_2 (see, e.g., minima D and E in Fig. 1). This condition guarantees that at low temperatures the system can switch between both minima without escaping to a third minimum. Tunneling systems correspond to DWPs with an asymmetry less than 1 K. DWPs can be easily identified from the 1D potential. In Fig. 4 they are marked by squares. Most of them have a distance $d^2 \ll 1$, and hence correspond to very close-by configurations. The data of Fig. 4 allow an estimation of the absolute number of tunneling systems in glasses. Having found 7 DWPs for 223 minima, one has a probability of $14/223$ per minimum that it belongs to a DWP. Hence a configuration with $32 \times 223/14 \approx 500$ particles on average contains one DWP. The average asymmetry of the observed DWPs is of the order $\bar{A} = 0.005 \times E_{\mathrm{cryst}} \approx 1.0$. For the example of NiP, a binary glass-forming system, the LJ energy scale corresponds to 1000 K and the distance scale to approximately 2 Å [9]. If one assumes that the asymmetry of DWPs is equally distributed, one roughly has one tunneling system per $500 \times (1000\ \mathrm{K}/1\ \mathrm{K}) \times \bar{A} \approx 5 \times 10^5$ particles, yielding a density of $2 \times 10^{46}\ \mathrm{J}^{-1}\,\mathrm{m}^{-3}$. This value is of the right order of magnitude if compared with experimental data on molecular [33] or metallic glasses [34].

In conclusion, a "topographic view of supercooled liquids" [14] can indeed be very helpful in explaining properties of glass-forming systems beyond their liquid regime. Specifically, properties of the melting, the glass transition, and the low-temperature anomalies can be obtained from quantitative knowledge of the energy landscape. The 1D representation stresses the common origin of the low-temperature anomalies and the glass transition. One expects that the complexity of the energy landscape dramatically increases with further increasing system size. However, this work shows that already very small model systems contain relevant information about the nature of real glass-forming systems.

I gratefully acknowledge helpful discussions with S. Büchner, H. W. Spiess, and R. Schilling, and the referee for constructive suggestions. This work is partially supported by the SFB 262.

[1] W. A. Phillips, J. Low. Temp. Phys. **7**, 351 (1972).
[2] P. W. Anderson, B. I. Halperin, and C. M. Varma, Philos. Mag. **25**, 1 (1972).
[3] A. Heuer and R. J. Silbey, Phys. Rev. Lett. **70**, 3911 (1993).
[4] H. R. Schober, C. Oligschleger, and B. B. Laird, J. Non-Cryst. Solids **156–158**, 965 (1993).
[5] M. Goldstein, J. Chem. Phys. **51**, 3728 (1969).
[6] G. Adam and J. H. Gibbs, J. Chem. Phys. **57**, 470 (1972).
[7] F. H. Stillinger and T. A. Weber, Phys. Rev. A **28**, 2408 (1983).
[8] S. A. Brawer, J. Chem. Phys. **81**, 954 (1984).
[9] T. A. Weber and F. H. Stillinger, Phys. Rev. B **32**, 5402 (1985).
[10] H. Bässler, Phys. Rev. Lett. **58**, 767 (1987).
[11] F. H. Stillinger, Phys. Rev. B **41**, 2409 (1990).
[12] U. Moanty, I. Oppenheim, and C. H. Taubes, Science **266**, 425 (1994).
[13] J. C. Dyre, Phys. Rev. B **51**, 12 276 (1995).
[14] F. H. Stillinger, Science **267**, 1935 (1995).
[15] S. S. Plotkin, J. Wang, and P. G. Wolynes, Phys. Rev. E **53**, 6271 (1996).
[16] F. L. Somer, Jr. and J. Kovac, J. Chem. Phys. **101**, 6216 (1996).
[17] K. D. Ball *et al.*, Science **271**, 963 (1996).
[18] A. Ansari *et al.*, Proc. Natl. Acad. Sci. U.S.A. **82**, 5000 (1985).
[19] W. Götze and L. Sjörgen, Rep. Prog. Phys. **55**, 241 (1992).
[20] C. A. Angell, J. Non-Cryst. Solids **131–133**, 13 (1991).
[21] M. Cieplak and J. Jäckle, Z. Phys. B **66**, 325 (1987).
[22] C. J. Tsai and K. D. Jordan, J. Phys. Chem. **97**, 11 227 (1993).
[23] R. S. Berry, Chem. Rev. **93**, 2379 (1993).
[24] R. S. Berry and R. Breitengraser-Kunz, Phys. Rev. Lett. **74**, 3951 (1995).
[25] R. E. Kunz and R. S. Berry, J. Chem. Phys. **103**, 1904 (1995).
[26] J. M. Grace and A. C. Anderson, Phys. Rev. B **40**, 1901 (1989).
[27] T. A. Weber and F. H. Stillinger, J. Chem. Phys. **80**, 2742 (1984).
[28] S. Buechner (private communication).
[29] A. Heuer and R. J. Silbey, Phys. Rev. B **48**, 9411 (1993).
[30] U. Buchenau, Yu. M. Galperin, V. L. Gurevich, and H. W. Schober, Phys. Rev. B **49**, 5039 (1991).
[31] As shown in Ref. [32], one explicitly obtains $\langle w_4^0 \rangle = 0.39 m v^2$ which, using $m v^2 \approx 0.5 f^{(2)}$ ($f^{(2)}$ being the second derivative of the pair interaction in the minimum) and $f^{(2)} a^2 \approx 67$ (in LJ units), yields $\langle w_4^0 \rangle \approx 10$.
[32] A. Heuer and R. J. Silbey, Phys. Rev. B **53**, 609 (1996).
[33] J. F. Berret and M. Meissner, Z. Phys. B **70**, 65 (1988).
[34] G. Bellessa, J. Phys. (Paris), Colloq. **41**, C8-723 (1980).